EXTREME ULTRAVIOLET EMISSION SPECTRUM OF CO_2 INDUCED BY ELECTRON IMPACT AT 200 eV

I. Kanik, J. M. Ajello and G. K. James

Jet Propulsion Laboratory, California Institute of Technology
Pasadena, CA 91109, USA

SUBMITTED TO:

CHEMICAL PHYSICS LETTERS
MARCH 11, 1993

Abstract

We present the extreme ultraviolet (EUV) emission spectrum of CO_2 induced by electron impact at 200 eV. There are 36 spectral features which are identified with a resolution of 0.5 nm over the wavelength range of 40 to 125 nm. Absolute emission cross sections were obtained for each of these features. The EUV emission spectrum induced by electron impact consist of atomic multiplets of CI,II and OI,II,III as well as CO and CO^+ molecular band systems produced by dissociative excitation. The CI (119.4 nm) multiplet is the strongest feature of CI with a peak cross section of 3.61×10^{-19} cm^2 at 200 eV. The strongest feature of OI in the EUV spectrum is the OI (99.0 nm) multiplet with a peak cross section of 3.59×10^{-19} cm^2 at 200 eV.

1. Introduction

We have completed a laboratory study of the extreme ultraviolet (EUV) emissions resulting from electron impact on CO_2 at 200 eV over the wavelength range from 40-125 nm. The emissions of CO_2 is of fundamental importance in the analysis of solar system observations by remote sensing UV instruments. In particular, the emission features produced by electron impact excitation of CO_2 are important in studying the upper atmospheres of Mars [1] and Venus[2] which have atmospheres dominated by CO_2. Future satellites will be equipped with EUV spectrometers, for example the planned EUV observatory, Lyman Explorer, and may make use of this new data for identification purposes from observations of stellar and interstellar UV spectra.

Barth et al. [1] reproduced the prominent UV and visible emission spectral features of the Mars dayglow in laboratory conditions by electron bombardment of CO_2. A laboratory study of the most prominent emission features produced by electron impact excitation of CO_2 in the FUV from 126-200 nm and MUV from 200-400 nm was completed by Ajello [3]. Mumma et al. [4] reported the VUV emission features resulting from dissociative excitation of CO_2 by electron impact. The dissociative excitation of CO_2 has also been studied by Sroka [5]. Freund [6] produced the a $^3\Pi$ state of CO by dissociative excitation of CO_2 by electron impact.

Spectroscopic analysis of CO_2 includes the work of Fox et al. [7] who found two band systems of CO_2^+ in the range 280-500 nm. Bueso-Sanllehi [8] analyzed the rotational lines of the 288.2-289.6 nm molecular band. At about the same time Mrozowski [9, 10, 11, 12] completed a study of the rotational lines of the $^2\Pi_u \rightarrow {}^2\Pi_g$ transition in the range 290-460 nm. Judge et al. [13] studied the $\tilde{A}\ ^2\Pi_u \rightarrow \tilde{X}\ ^2\Pi_g$ band system by photon excitation and reidentified some bands given in the vibrational designation (n,0,0) $\rightarrow$ (m,0,0) by Mrozowski as actually (n,0,0) $\rightarrow$ (m,0,2). Judge et al. [13] also showed that the (n,0,0) $\rightarrow$ (m,1,1) assignments are really (n,0,0) $\rightarrow$ (m,0,2) transitions. McConkey et al. [14] and Nishumura [15] measured the excitation cross sections for the $\tilde{A}\ ^2\Pi_u$ and $\tilde{B}\ ^2\Sigma^+$ band systems of CO_2^+ by electron impact in the energy range from threshold to 1 keV and 100 eV to 1 keV, respectively.

2. Experimental Procedure

The instrumentation and calibration techniques used in these measurements have been described in detail in earlier publications by Ajello et al. [16, 17, 18], Ajello and Shemansky [19], and Shemansky et al. [20,21]. In brief, the instrument consists of an electron impact emission chamber in tandem with two UV monochromators. A crossed beam configuration is employed to measure the electron impact emission cross sections. In a typical crossed-beam arrangement, a magnetically collimated,

monoenergetic beam of electrons intersects a beam of gas (CO_2) formed by capillary array at right angles under optically thin conditions. The background pressure can be varied from $5x10^{-8}$ to $3x10^{-4}$ T to ensure optically thin conditions. Emitted photons corresponding to the radiative decay of collisionally excited states of CO_2 are detected at 90^0 by a UV monochromator equipped with a channeltron detector. No corrections for polarization of the radiation are made. Polarization of the radiation is considered to be small where many rotational states contribute to a vibrational band for an excited molecule. The instrument is entirely automated for repetitive scans and interfaced with a computer. The static gas mode is used for the measurement of excitation functions.

The relative intensity calibration of the optical system and detector with wavelength is determined by two procedures in each wavelength region. Electron excited spectra of reference gases He, H_2, and Ar are used as EUV calibration sources. In detail, the relative sensitivity of the spectrometer is determined by comparing the measured strengths of the molecular or atomic features with synthetic spectra. The synthetic spectra are based on the instrumental spectral transmission function convolved with calculated discrete transitions [17]. The laboratory measurements together with the spectroscopic models permitted the EUV spectrum from H_2 Rydberg series to serve as relative calibration standards in the 80-230 nm range. For shorter wavelengths (40-80 nm) the $n^1\Pi^0$ n=2,3,4 Rydberg series of He and ArI,II multiplets are used as the calibration source [17]. The absolute energy scale for the electron beam was established by setting the voltage scale to the appearance potential for ArII (91.96nm) at 29.24eV.

The absolute cross section of OII (83.4 nm) emission produced by electron impact at 200 eV on CO_2 used to normalize the entire 200 eV EUV spectrum is determined by the relative flow technique [22,23]. The essence of the relative flow technique is to determine the absolute emission cross section of a gas with an unknown cross section in terms of the absolute cross section of a gas with a well known cross section. In this technique, the NI (119.99 nm) fluorescence signal at 200 eV impact energy from N_2, the standard gas, is compared to the fluorescence signal from the 83.4 nm emission produced by electron impact at 200 eV on CO_2, the unknown gas, at low background pressures in the molecular flow gas regime. The comparisons were made over a range of background gas pressures from 6×10^{-7} to 1×10^{-5} T to establish linearity of signal with pressure. Once the linearity of signal with pressure is established, we measure relative emission cross section for the 83.4 nm emission produced by electron impact at 200 eV on CO_2, $(Q_{rel})^{CO_2}$, then relative emission cross section for the 119.99 nm emission produced by electron impact at 200 eV on N_2, $(Q_{rel})^{N_2}$, with identical electron gun and detector conditions. We define the relative emission cross sections for CO_2 and N_2 according to the following formulas:

$$(Q_{rel})^{CO_2} = I^{CO_2} / (P \times I_e)^{CO_2} \qquad (1)$$

$$(Q_{rel})^{N_2} = I^{N_2} / (P \times I_e)^{N_2} \quad (2)$$

where I^{CO_2} and I^{N_2} are the signal intensities for CO_2 and N_2 respectively and P is the background pressure and I_e is the electron beam current collected in the Faraday cup. The absolute emission cross section, $(Q_{ABS})^{CO_2}$, for CO_2 (in this case for 83.4 nm feature) is then determined based on the following formula:

$$(Q_{ABS})^{CO_2} = (Q_{rel})^{CO_2} \times [(Q_{ABS})^{N_2} / (Q_{rel})^{N_2}] \quad (3)$$

where a value of 31.1×10^{-19} cm^2 was used as the absolute cross section ($(Q_{ABS})^{N_2}$) for NI (119.99 nm) production by dissociative excitation of N_2 at 200 eV [24].

We judge the root sum square uncertainty in the absolute cross sections given in this work is approximately 22% based on the uncertainties in the NI (119.99 nm) cross section, relative calibration and signal statistics.

3. Results

Fig.1 shows the CO_2 extreme ultraviolet (EUV) laboratory spectrum at 200 eV electron impact energy. The EUV emission spectrum of CO_2 at 200 eV impact energy consists of 36 spectral features identified at a resolution of 0.5 nm over the wavelength range of 40-120 nm. All the emission features can be attributed to the process of dissociative excitation. Further studies have been conducted at wavelengths which are particularly strong for each type of atomic fragment. The spectral features are composed of atomic multiplets of CI,II and OI,II,III as well as CO and CO^+ molecular band systems. Table 1 lists the candidate identifications of the blended atomic and molecular spectral components that contribute to each feature at this resolution, together with the measured emission cross section at 200 eV. The atomic multiplet identifications are taken from Kelly [25]. The molecular features are identified from the work of James et al. [26]. The relative cross sections for each feature given here were obtained by integrating the signal intensity over the wavelength interval for the feature of interest and then by normalizing the integrated signal intensity for each spectral feature to 83.4 nm spectral feature by comparing its area relative to the area of the 83.4 nm feature. The absolute cross sections of all the spectral features were determined by using the absolute cross sections of 83.4 nm feature whose cross section had been determined by the relative flow technique described above.

In addition to the electron excited CO_2 spectrum at 200 eV, we have acquired excitation functions for emission features at wavelengths 83.4 nm and 99.0 nm which are particularly strong and well resolved from OII and OI atomic fragments, respectively. Two different energy ranges were independently scanned for each of the features mentioned above: a) the threshold region (typically 0-400 eV) and b) the Bethe-Born region(typically 0-1000 eV). These cross section curves are shown in Fig. 2 and Fig. 3 for the 83.4 nm and 99.0 nm features respectively. It is important to separate the underlying dissociation channels. For example the basic processes of lowest dissociation energy which can be observed in single collisions of electrons and CO_2 leading to the emission of photons are:

1. $CO_2 + e \rightarrow CO + O^* + e$, dissociative excitation,

2. $CO_2 + e \rightarrow C + O^* + O + e$, dissociative excitation,

3. $CO_2 + e \rightarrow CO^+ + O^* + 2e$, dissociative ionization excitation,

4. $CO_2 + e \rightarrow C^+ + O^* + O + 2e$, dissociative ionization excitation, and

5. $CO_2 + e \rightarrow C + O^* + O^+ + 2e$, dissociative ionization excitation.

Similar equations can be written for OII, CI, CII excited fragments observed in this experiment.

The CI features are singlets and triplets, the CII features are doublets and quartets. Similarly, the OI features are singlets and triplets (except for the long-lived $^5S^o \rightarrow$ g ^3P transition), the OII features are doublets and quartets [25]. The 83.4 nm OII feature contains a small contribution from the OIII resonance transition at nearly the same wavelength. The strongest feature of OI in the EUV spectrum of CO_2 is the OI (99.0 nm) multiplet with a peak cross section of 3.59 x 10^{-19} cm^2 at 200 eV. The CI (119.4 nm) multiplet is the strongest feature of CI with a peak cross section of 3.61 x 10^{-19} cm^2 at 200 eV in the EUV spectrum of CO_2.

4. Conclusion

We have presented the EUV emission spectrum of CO_2 induced by electron impact at 200 eV over the wavelength range from 40-120 nm. Absolute emission cross sections were obtained for each of 36 identified features. The emission spectrum consists of atomic multiplets of CI, CII, OI, OII, and OIII as well as CO and CO^+ molecular band systems. The root sum square uncertainty in the absolute cross sections is estimated to be 22%. We also obtained the oscillator strength for the 83.4 nm and 99.0 nm features.

5. Acknowledgment

The research described in this publication was carried out at the Jet Propulsion Laboratory, California Institute of Technology and Sponsored by the Air Force Office of Scientific Research (AFOSR), the Aeronomy Program of the National Science Foundation under grant ATM 8715709, and the NASA Planetary Atmospheres, Space Physics and Astronomy Program Offices through an agreement with the National Aeronautics and Space Administration.

References

[1] C. A. Barth, W. G. Fastie, C. W. Hord, J. B. Pearce, K. K. Kelly, A. I. Steward, G. E. Thomas, G. P. Anderson, and O. F. Raper, Science **165** (1969) 1004.

[2] A. I. F. Stewart, Astron. Astrophys. **187** (1987) 369.

[3] J. M. Ajello, J. Chem. Phys. **55** (1971) 3169.

[4] M. J. Mumma, E. J. Stone, W. L. Borst, and E. C. Zipf, J. Chem. Phys. **57** (1972) 68.

[5] W. Sroka, Z. Naturforsch **25** (1970) 1434.

[6] R. S. Freund, J. Chem. Phys. **47** (1967) 2897.

[7] G. W. Fox, O. S. Duffendack, and E. F Barker, Proc. Natl. Acad. Sci. (U.S.) **13** (1927) 302.

[8] F. Bueso-Sanllehi, Phys. Rev. **60** (1941) 556.

[9] S. Mrozowski, Phys. Rev. **60** (1941) 730.

[10] S. Mrozowski, Phys. Rev. **62** (1942) 270.

[11] S. Mrozowski, Phys. Rev. **72** (1947) 682.

[12] S. Mrozowski, Phys. Rev. **72** (1947) 691.

[13] D. L. Judge, G. S. Bloom, and A. L. Morse, Can. J. Phys. **47** (1969) 489.

[14] J. W. McConkey, D. J. Burns, and J. M. Woolsey, J. Phys. B **1** (1968) 71.

[15] H. Nishimura, J. Phys. Soc. Japan **24** (1968) 130.

[16] J. M. Ajello, D. E. Shemansky, T. L. Kwok, and Y. L. Yung, Phys.Rev. **29** (1984) 636.

[17] J. M. Ajello, D. E. Shemansky, B. Franklin, J. Watkins, S. Srivastava, G. K. James, W. T. Simms, C. T. Hord, W. Pryor, W. McClintock, V. Argabright, and D. T. Hall, Appl. Opt. **27** (1988) 890.

[18] J. M. Ajello, G. K. James, B. O. Franklin, and D. E. Shemansky, Phys. Rev. A **40** (1989) 3524.

[19] J. M. Ajello and D. E. Shemansky, J. Geophys. Res. **90** (1985) 9845.

[20] D. E. Shemansky, J. M. Ajello, and D. T. Hall, Ap. J. **296** (1985) 765.

[21] D. E. Shemansky, J. M. Ajello, D. T. Hall, and B. Franklin, Ap. J. **296** (1985) 774.

[22] S. K. Srivastava, A. Chutjian and S. Trajmar, J. Chem. Phys. **63** (1975) 2659.

[23] J. C. Nickel, C. Mott, I. Kanik and D. C. McCollum, J. Phys. B **21**, (1988) 1867.

[24] G. K. James, J. M. Ajello, B. Franklin, and D. E. Shemansky, J. Phys. B **23** (1990) 2055.

[25] R. L. Kelly, Atomic and Ionic spectrum lines below 2000 angstroms: Hydrogen through krypton-Part I (H-Kr), J. Chem. Ref. Data **16** (1987) 35.

[26] G. K. James, J. M. Ajello, I. Kanik, B. Franklin and D. E. Shemansky, J. Phys. B **25** (1992) 1481.

TABLE 1. Emission Cross Sections of CO_2 at 200 eV

Feature Number	Species	Wavelength λ (nm)	Observed Peak λ (nm)	Emission Cross Section (cm^2)
1.	O II	48.16 - 48.56	48.3	2.15×10^{-20}
2.	C II O II	51.66 - 51.71 51.55 - 51.82	51.7	1.59×10^{-20}
3.	C II O II	53.17 - 54.34 53.78 - 53.98	53.9	9.19×10^{-20}
4.	C II O II	54.93 - 56.47 55.50 - 55.51	55.4	4.54×10^{-20}
5.	C II O II	59.48 - 60.05 60.06	60.1	3.93×10^{-20}
6.	O II	60.31 - 61.71	61.7	5.57×10^{-20}
7.	C II O II CO^+	64.16 - 65.14 64.12 - 64.41 63.44 - 65.77	64.5	3.71×10^{-20}
8.	O I O II CO CO^+	66.70 - 66.75 67.29 - 67.38 66.84 - 67.57 67.07 - 67.24	67.3	1.68×10^{-20}
9.	C II O I C O	68.64 - 68.73 68.55 - 68.82 68.32 - 69.09	68.8	1.68×10^{-20}
10.	O I O II $C O^+$	72.48 - 72.61 71.85 - 71.86 71.67	71.9	6.86×10^{-20}
11.	C II O I $C O^+$	80.64 - 80.98 80.43 - 81.69 81.08	80.7	4.31×10^{-20}
12.	O II O III	83.28 - 83.45 83.29 - 83.53	83.4	1.78×10^{-19}
13.	C II O I O II	85.81 - 85.86 85.93 - 86.44 85.93 - 86.03	85.8	5.37×10^{-20}
14.	O I $C O^+$	87.78 - 88.29 87.38 - 88.48	87.9	6.45×10^{-20}
15.	C II C O $C O^+$	90.36 - 90.45 89.67 - 90.96 89.80 - 90.84	90.5	1.04×10^{-19}
16.	O I	91.20 - 92.74	92.3	4.7×10^{-20}
17.	O I C O $C O^+$	92.95 - 93.98 93.00 - 93.99 93.83	93.7	7.06×10^{-20}

Feature Number	Species	Wavelength λ (nm)	Observed Peak λ (nm)	Emission Cross Section (cm^2)
18.	C I C II O I	94.52 - 94.56 94.60 - 94.62 95.09 - 95.29	95.0	4.87×10^{-20}
19.	O I C O	95.98 95.61 - 96.05	95.8	1.04×10^{-20}
20.	O I O II C O	97.17 - 98.08 97.13 96.44 - 97.75	97.3	1.54×10^{-19}
21.	O I C O	98.86 - 99.08 98.27 - 98.93	99.0	3.59×10^{-19}
22.	O I C O	99.95 100.25 - 100.27	100.0	3.35×10^{-20}
23.	C II O II C O	100.99 - 101.04 100.90 - 101.06 101.09 - 101.18	101.1	0.39×10^{-20}
24.	O I C O	102.58 - 102.89 101.79 - 102.93	102.7	3.06×10^{-19}
25.	C II O I C O	103.63 - 103.70 103.92 - 104.29 103.46 - 103.97	103.9	1.56×10^{-19}
26.	C II C O	106.33 - 106.61 106.309	106.5	0.70×10^{-20}
27.	C II O II C O	109.19 - 109.27 107.83 - 107.92 107.61 - 108.79	108.0	8.19×10^{-20}
28.	C I O I	110.42 - 111.28 110.52	110.5	8×10^{-20}
29.	C I C O	111.52 - 112.90 112.36	112.0	7.16×10^{-20}
30.	C I C O	112.91 - 113.02 113.25	113.1	7.56×10^{-20}
31.	C I C II C O	113.84 - 114.16 113.89 - 114.17 113.97	114.1	8.62×10^{-20}
32.	C I O I C O	115.58 - 115.97 115.22 115.13 - 115.15	115.2	3.43×10^{-19}
33.	C I C O	118.88 - 119.79 118.01 - 118.61	119.4	3.61×10^{-19}
34.	O I	121.76	121.5	5.43×10^{-20}

Feature Number	Species	Wavelength λ (nm)	Observed Peak λ (nm)	Emission Cross Section (cm^2)
35.	C I C O	124.13 - 124.23 122.98	123.5	1.84×10^{-19}
36.	C I	124.13 - 124.79	124.5	2.49×10^{-20}

Figure Captions

Figure 1. The EUV spectrum of electron impact induced fluorescence of CO_2 at 200 eV. The EUV spectrum calibrated for instrument sensitivity is obtained at a spectral resolution of 0.5nm from 40 to 120nm. The feature numbers are listed in Table 1 with identifications and cross sections.

Figure 2. Relative emission cross section of the 83.4nm multiplet feature number 12 from ionization excitation of CO_2. The top half of the figure shows data points every 0.391 eV from 0-400eV and shows the important threshold energies. The bottom half of the figure shows data points spaced every 1.042 eV from 0-1000eV.

Figure 3. Relative emission cross section of the 99.0nm multiplet feature number 21 from dissociative excitation of CO_2 . The top half of the figure shows data points every 0.391 eV from 0-400eV and shows important threshold energies. The bottom half of the figure shows data points spaced every 1.042eV from 0-1000 eV.

Figure 1

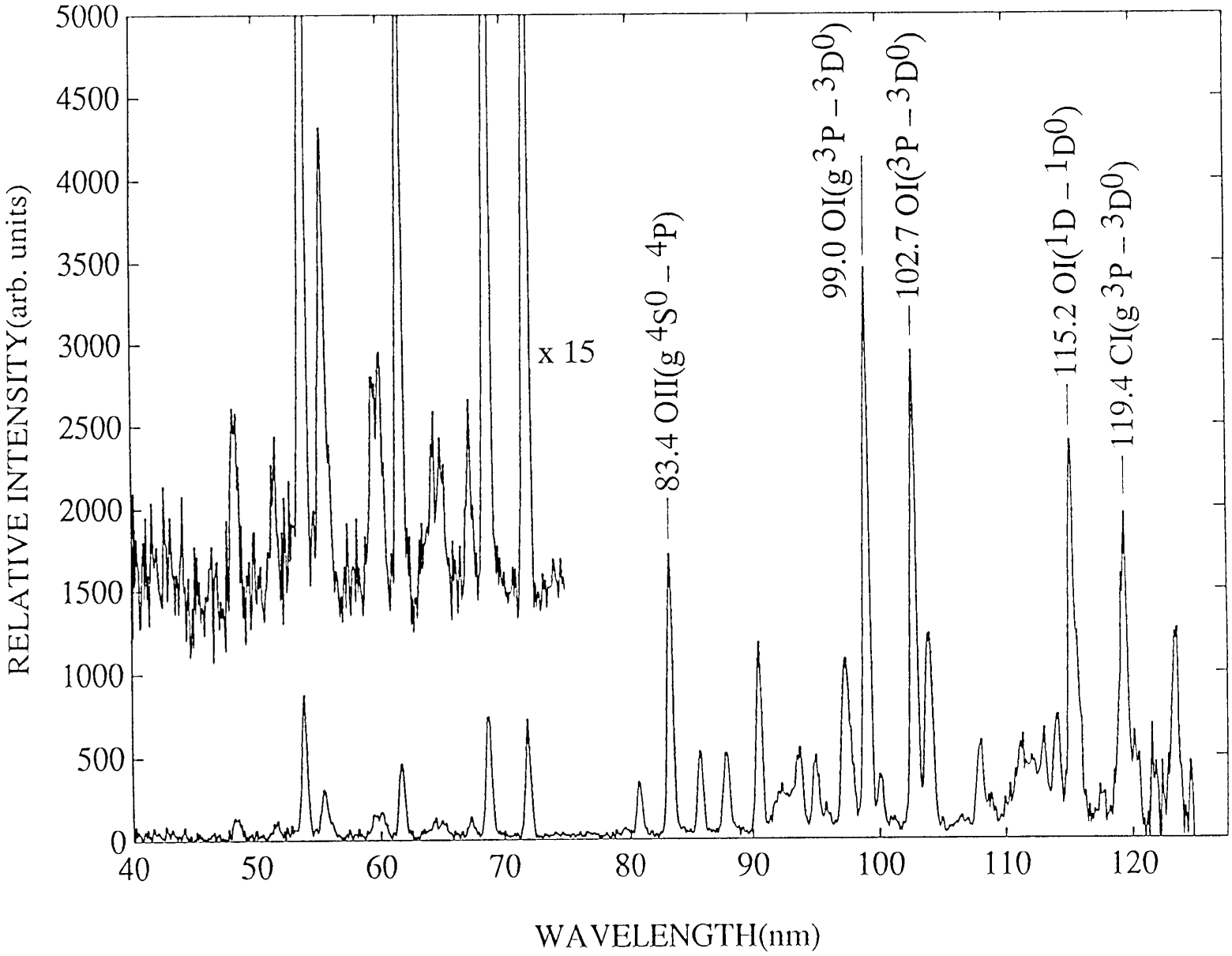
RELATIVE INTENSITY(arb. units)
WAVELENGTH(nm)
x 15
83.4 OII(g 4S0 – 4P)
99.0 OI(g 3P – 3D0)
102.7 OI(3P – 3D0)
115.2 OI(1D – 1D0)
119.4 CI(g 3P – 3D0)
0
500
1000
1500
2000
2500
3000
3500
4000
4500
5000
40
50
60
70
80
90
100
110
120

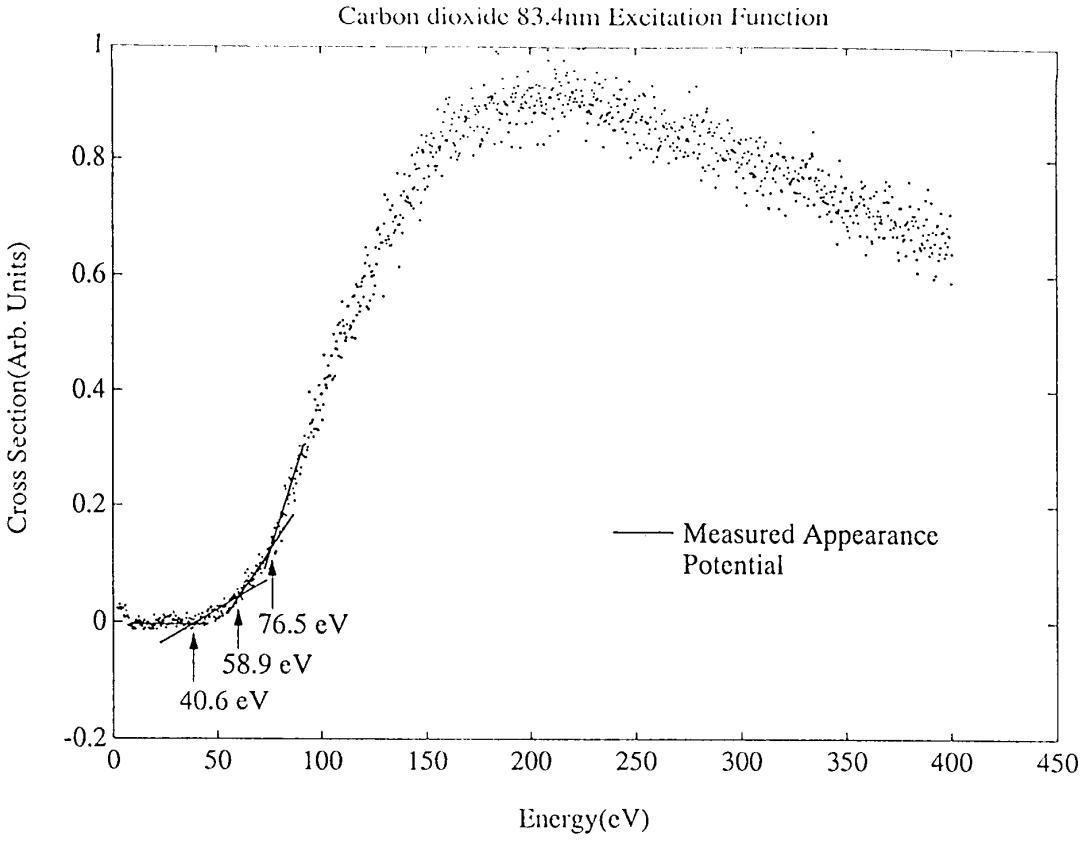
Carbon dioxide 83.4nm Excitation Function
Cross Section(Arb. Units)
Energy(eV)
Measured Appearance Potential
76.5 eV
58.9 eV
40.6 eV
1
0.8
0.6
0.4
0.2
0
-0.2
0
50
100
150
200
250
300
350
400
450

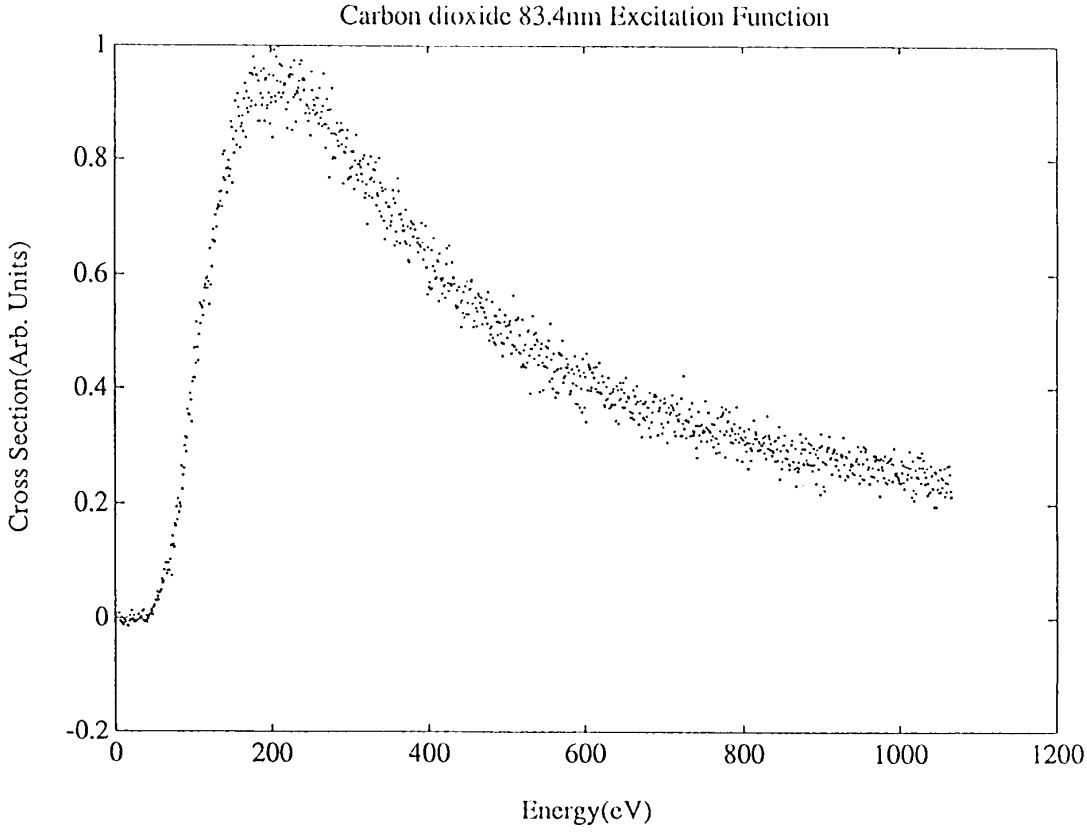
Carbon dioxide 83.4nm Excitation Function
Cross Section(Arb. Units)
Energy(eV)
1
0.8
0.6
0.4
0.2
0
-0.2
0
200
400
600
800
1000
1200

Figure 2

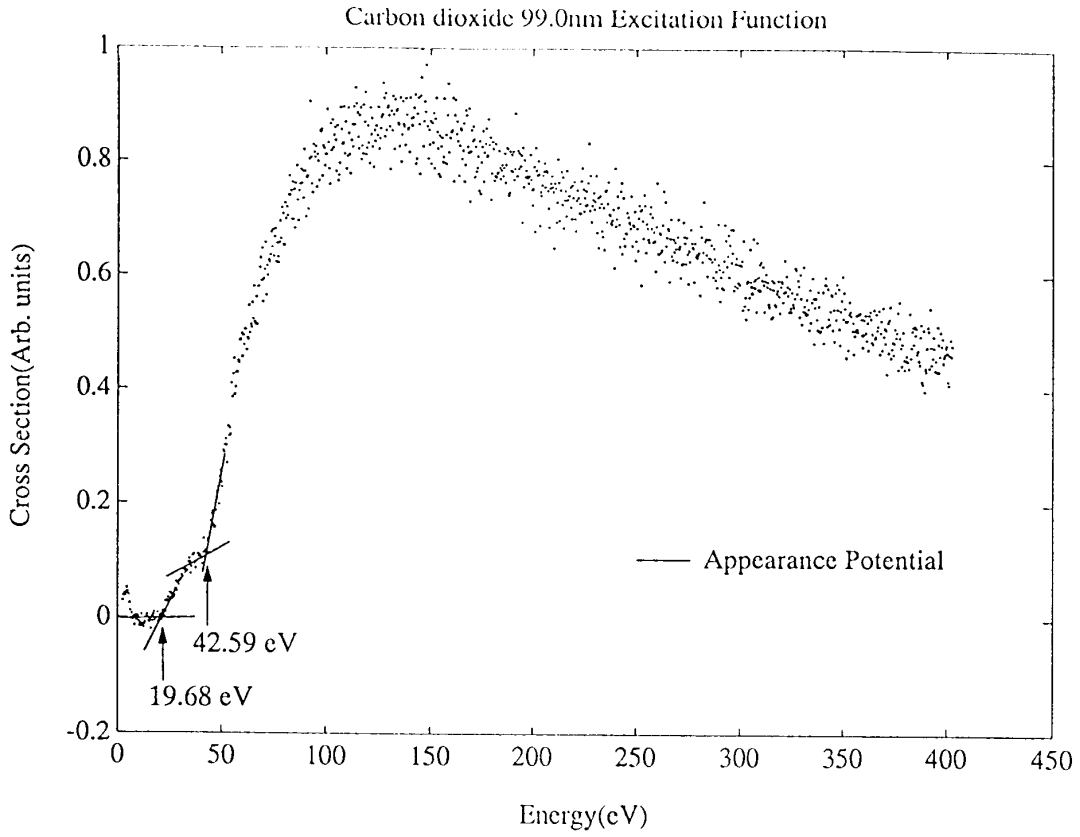
Carbon dioxide 99.0nm Excitation Function
Cross Section(Arb. units)
Energy(eV)
Appearance Potential
42.59 eV
19.68 eV
1
0.8
0.6
0.4
0.2
0
-0.2
0
50
100
150
200
250
300
350
400
450

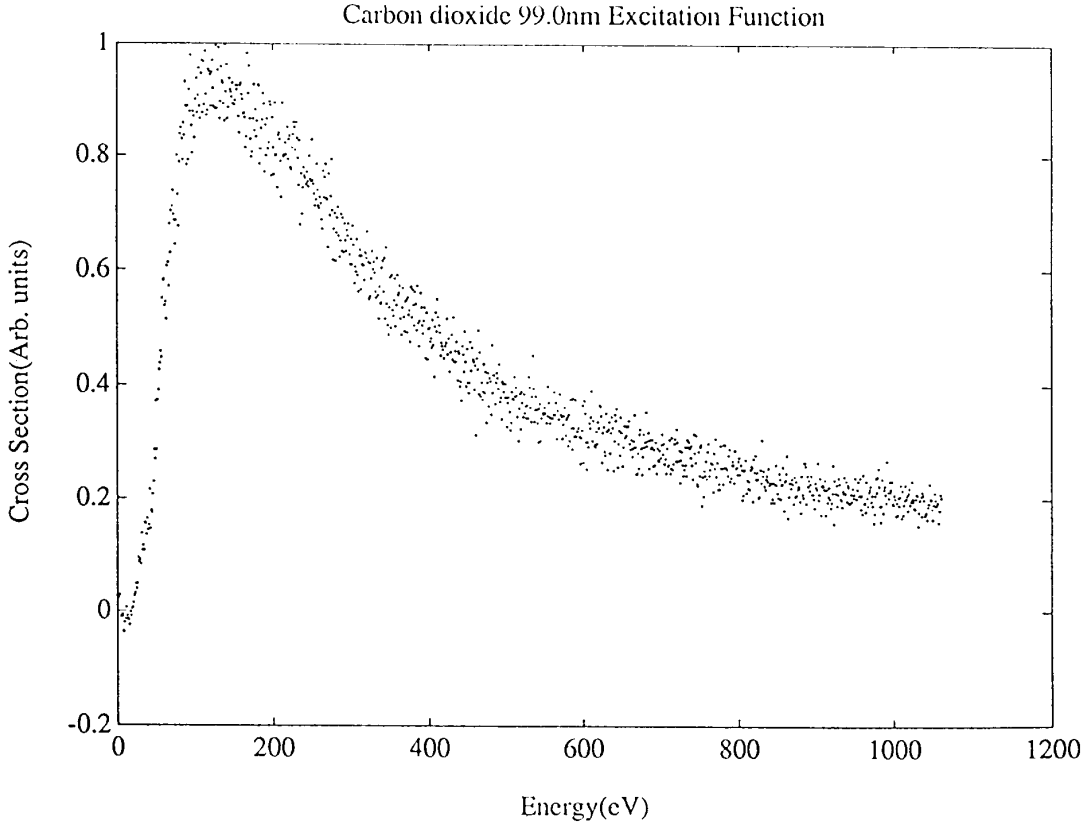
Carbon dioxide 99.0nm Excitation Function
Cross Section(Arb. units)
Energy(eV)
1
0.8
0.6
0.4
0.2
0
-0.2
0
200
400
600
800
1000
1200

Figure 3